Assessment of different control strategies to manage cloud-induced transients in central receiver systems using molten salts

Cite as: AIP Conference Proceedings **2033**, 040038 (2018); https://doi.org/10.1063/1.5067074
Published Online: 08 November 2018

Andrea Toscani, Francesco Crespi, David Sánchez, Marco Binotti, and Giampaolo Manzolini

Assessment of Different Control Strategies to Manage Cloud-Induced Transients in Central Receiver Systems Using Molten Salts

Andrea Toscani[1,2], Francesco Crespi[1], David Sánchez[1], Marco Binotti[2,a] and Giampaolo Manzolini[2]

[1]*Thermal Power Group (GMTS), University of Seville, Camino de los Descubrimientos s/n, Seville, 41092, Spain.*
[2] *Group of Energy Conversion Systems (GECOS), Politecnico di Milano, Via Lambruschini 4, Milano, 20156, Italy.*

[a)] Corresponding author: marco.binotti@polimi.it

Abstract. This paper presents an assessment of different control strategies to be applied in central receiver systems operating with molten salts. The objective is to identify the best control scheme to achieve a threefold objective: (i) to ensure that the outlet temperature of the receiver remains at the highest possible value, (ii) to guarantee that the temperature limit of the working fluid is not exceeded, and (iii) to minimize the temperature gradients induced in the pipes. The analysis is performed in a reference plant whose main specifications are taken from *Gemasolar*, located in Fuentes de Andalucía (Seville, Spain). The model of the solar receiver and the configuration of the clouds have been presented in previous works by the authors. This work moves one step forward, focusing on the thermal performance of the receiver under different flow management strategies. Two classical control schemes are adopted in this work: *feed-forward* and *feed-back*. The latter, improved with a variable *under-relaxation* factor *K,* is found to be the best choice in order to guarantee safe operation. It yields a lower maximum temperature gradient than the *feed-forward* scheme and it also ensures that the outlet temperature is always within the limits that avoid degradation of the working fluid (600ºC). Regarding the worst cloud scenario, *Total Shadow* results to be the most demanding case requiring complete shut-down of the pumping station, at which point the power plant operates on the storage system only.

INTRODUCTION AND PREVIOUS STUDIES

The present manuscript belongs to a wider research pathway developed thanks to the collaboration between University of Seville and Politecnico di Milano. A series of studies have been made in the last few years and have been used to obtain the results presented here. The aiming strategy of the heliostats was originally investigated in [1], in order to find the best solution capable of reducing the thermal stresses of the receiver without affecting the production of electric power. The main feature of this aiming strategy is to spread the incoming heat flux onto the whole receiver surface, reducing the peak temperature and associated thermal gradients [1]. Later, a quasi-steady state analysis of the optical performance of the solar field was made, considering the off-design conditions caused by the passage of clouds [2]. In the present manuscript five of these cloud schemes are considered, as shown in Fig. 1: *Total Shadow* (a), a big cloud covering the entire Gemasolar solar field; *Small Cloud* (b), a cloud of about 200 m passing across the centerline of the field; *Total Shadow as PS10* (c), a cloud with the size of the solar field of the PS10 power plant, originally used to compare both plants; *Left Shadow as PS10* (d) similar to the previous cloud but covering the left part of the field only; *Two Small Clouds* (e), two parallel clouds passing across the middle of the field, similarly to the *Small Cloud* case. In this analysis, a cloud speed of 10 m/s is considered and the progressive covering of the field is modeled as a series of steady-state conditions, dividing the entire process in 20 time-steps. This assumption is made in order to have a good compromise between accuracy and computational cost of the simulation. The main conclusion of this optical analysis is that the *Total Shadow* always leads to the worst scenario for the solar receiver, due to its large size and to the fact that it covers the entire field. Nevertheless, it is also worth noting that clouds

SolarPACES 2017
AIP Conf. Proc. 2033, 040038-1–040038-8; https://doi.org/10.1063/1.5067074
Published by AIP Publishing. 978-0-7354-1757-1/$30.00

presenting largely different sizes can produce similar effects, depending on which parts of the field they are covering [2]. Finally, the off-design performance of the solar receiver was studied in [3], confirming the results previously obtained. The receiver model is constituted by a total of 432 pipes, which are divided in 28 vertical segments (j-index), furtherly subdivided in 8 circumferential pieces (i-index). For sake of simplicity, the pipes are assembled in 18 panel collectors, so that the HTF entering in each panel pipes comes from the previous panel collector and, as a consequence, has the same temperature profile. This circumstance allows to ease the complexity of the problem considering only 18 pipes, one for each of the 18 panel collectors (p-index). The three indexes (i,j and p) are the ones hereby considered in Eq. 4. The complete in-house model used in the transient thermal performance analysis is provided in [3]. In the present paper, the tests are performed on March 20 at 12 a.m., a day characterized by a DNI of 970 kW/m^2 and a solar field mean optical efficiency of 62.5%.

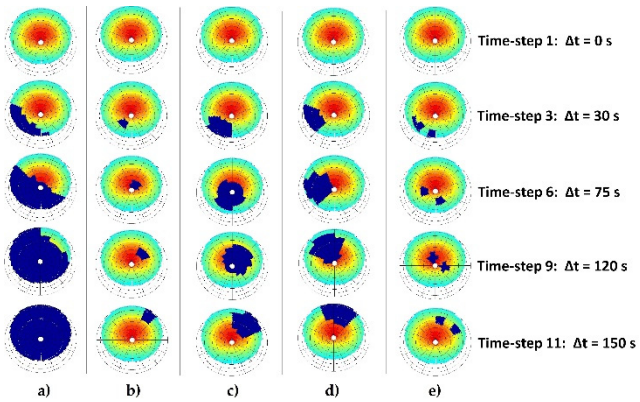

FIGURE 1. Shadowing of the solar field as a consequence of the different cloud schemes. Clouds are coming from the S-W corner of the field.

CONTROL SYSTEM - THEORETICAL BASIS

The control system is a fundamental element for a solar receiver as it ensures that the target conditions of the heat transfer fluid at the outlet of the receiver are always met, mitigating the risks related to mechanical integrity. This is usually accomplished by acting on the HTF mass flow rate; in summary: for constant incident radiation, the higher the mass flow rate sent to the receiver pipes, the lower the HTF temperature at the outlet section, whereas the opposite holds true for a reduction of the mass flow rate.

Feed Forward Control

A *feed-forward* control scheme acts on a particular system in a predefined way according to a measured parameter and a corrective map (*lookup table*) provided in advance; i.e., starting from a measured parameter, the method is able to provide a corrective action $u(t)$ according to a set of predefined values available in a *lookup table*. Once the corrective action takes place, it is possible to check the result obtained with respect to the target one. The resulting method is very simple and requires a lower computational load with respect to the *feed-back* approach, but it is not able to control the system if the current scenario is not well described in the predefined *lookup table*.

From a practical standpoint, the control system is made up of a pyranometer and an electronic circuit board-linked to the HTF pump. The former measures the solar radiation that reaches the receiver surface for each time-step and provides this information to the electronic circuit board. Based on this information from the pyranometer, the latter computes the amount of HTF mass flow that the pump has to send to the receiver circuits by interpolation of the data available in the *lookup table*. The mass flow rate of molten salts is hence proportional to the incoming radiation for each time-step along the complete passage of the cloud.

The *lookup table* is easily calculated by considering a number of radiation maps, for each one of which the mass flow rate of HTF needed to run the receiver at the rated outlet temperature under stationary conditions is computed. In this way, once the average incident radiation is measured, the code can autonomously compute the flow rate of molten salts and provide a transient solution for each time step. In addition to this, the model developed complements the traditional feed forward calculation with a further correction that is proportional to the error in the previous time

step. This makes it possible to create a more sensitive controller able to respond to the thermal oscillations of the system. K is the under-relaxation factor with respect to the error e in the previous time step $(t-1)$: $e(t-1)$.

The control logic of the whole model is explained in Fig. 2. Note that "transient thermal model" refers to the in-house code modelling the performance of the solar receiver. For each time-step, the code measures the average incoming radiation and computes the correspondent value of the HTF mass flow rate through the *lookup table*. Once initialized with the values set by the control system, the transient thermal model is run and provides the temperatures of both the molten salts and the pipe wall temperatures. The error between the target and the real (measured) HTF outlet temperature is computed by the controller and the result is saved for the next time-step correction.

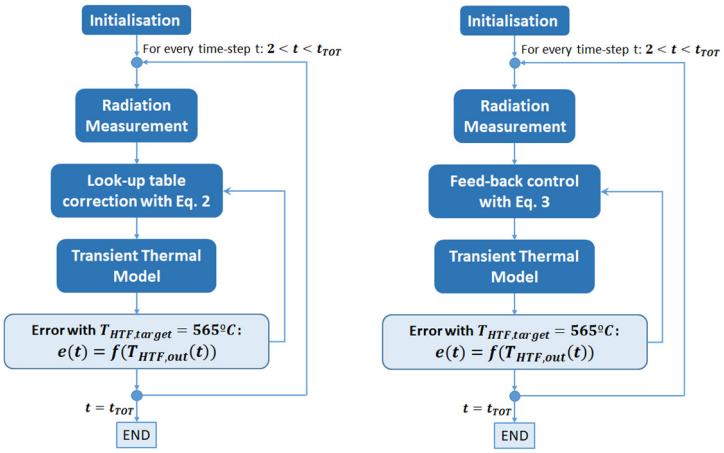

FIGURE 2. Control system with *feed-forward* (left) and *feed-back* (right) operating principle. Eq.2 and Eq.3 refers to equation numbering in the text.

The results obtained when applying the model to the transient problem are reported in Fig. 3, where the best K coefficients found for the cases of high and low error influence have been used. High values of K mean that greater importance is given to the error computed in the previous time-step and, as a consequence, the corrective actions on $\dot{m}_{fluid\ tot}$ provided by the *lookup table* are more aggressive/abrupt according to Eq. 1. This is a more *pessimistic* perspective in which *lookup table* values are considered less reliable and the system has a higher degree of freedom regulating the HTF mass flow rate by itself according to the computed error. On the contrary, low values of K are used if lower importance is given to the error computed in the previous time-step and, as a consequence, the $\dot{m}_{fluid\ tot}$ value results to be almost equal to the one provided by the *lookup table*. In this case, the *lookup table* is considered with a higher level of confidence.

$$\dot{m}_{fluid\ tot}(t) = \dot{m}_{lookup\ table}(t) \cdot \left(1 - K \cdot e(t-1)\right) \tag{1}$$

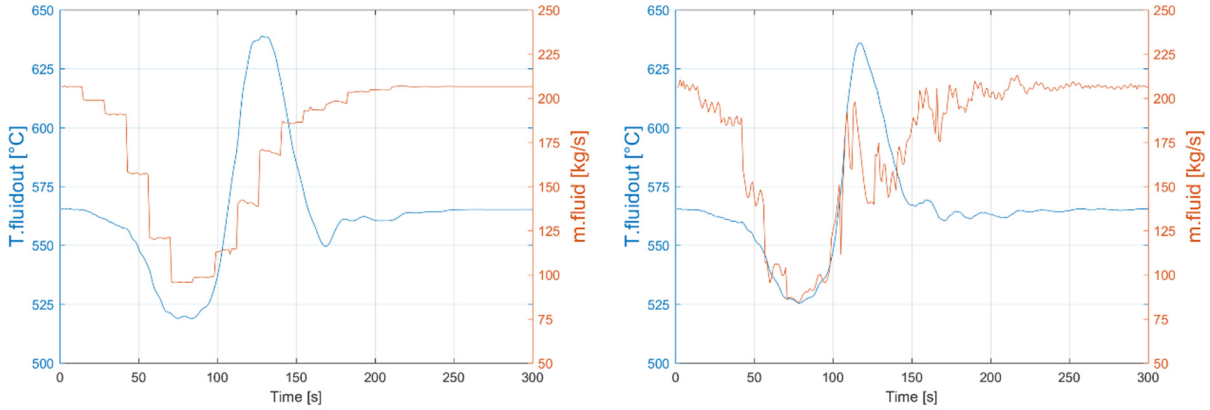

FIGURE 3. *Total shadow as PS10* cloud transient performance using low K (left) and high K (right) control systems. HTF mass flow in orange and HTF outlet temperature in blue.

The two proposed solutions for the *Total Shadow as PS10* passage are very similar despite having used different values of K. The main difference is found for the mass flow rate of HTF (shown in orange): for the high K case, a more oscillating trend is detected, whereas the curve follows a step-like behavior for the low K. Both curves show local minimum and maximum outlet temperatures brought about by the lack of incoming radiation when the shadow of the cloud is largest. In this regard, even if adopting high K leads to a better control of the maximum value. neither of the two proposed solution seems to comply with to the upper degradation limit (600ºC) fully. In fact, as the cloud starts to leave the solar field and the total incoming radiation rises, the control system is not able to properly control the maximum fluid temperatures through a parallel increase of HTF mass flow. As a consequence, degradations issues are likely to appear due to excessive fluid temperature. It is obvious to conclude that the problems related to the arrival of the cloud are less critical since it is the unshadowing of the solar field which poses the most demanding operating conditions on the system. The *feed-back* scheme is now explored to check if it provides better controllability.

Feed Back Control

In a *feed-back* control, the corrective action is based on the current state of the project and not in the foreseen variables. Although various type of *feed-back* control schemes are available in literature, a PID controller has been selected for the present model [4]. This identifies a controller that includes element able to provide three function in the system control task: proportional, integral and derivative. A PID controller continuously calculates an error value $e(t)$ as the difference between a desired set point and a measured process variable and applies a correction based on proportional, integral, and derivative terms. The controller attempts to minimize the error over time by adjustment of a control variable $u(t)$ to a new value determined by a weighted sum of the PID terms:

$$u(t) = K_P \cdot e(t) + K_I \cdot \int_0^t e(\tau)\, d\tau + K_D \cdot \frac{d[e(t)]}{dt} \tag{2}$$

where K_P , K_I , and K_D, represent the coefficients for the proportional, integral, and derivative terms respectively. Particular attention has to be focused in the PID coefficients since extreme values of these (either too low or too high) can affect the system response negatively. For instance, a high proportional gain K_P can result in a large change in the output for a given error, leading to an unstable system. On the other hand, a small gain produces a small corrective action even in case of a large input error, characterizing a less responsive and less sensitive controller. Also if the proportional gain is too low, the control action may be too small when responding to system disturbances. Therefore, the main issue is to find the specific values of K_P, K_I, and K_D through which the model response for any cloud passage can be controlled stably.

This control system is constituted by a thermocouple and an electronic circuit board linked to the HTF pump. The thermocouple measures the HTF temperature at the outlet section for every time-step and provides this information to the electronic circuit board. The latter takes this information and computes the HTF mass flow to be pumped by the to the receiver piping according to the error between the measured and target values. In the evaluation of the new mass flow rate, each PD components is taken into account together with the previous time-step error $[e(t\ -\ 1)]$. It is worth noting that the control system had the three PID terms originally but it was later modified to adopt PD components only, due to the instabilities introduced in the system by the integral element.

$$\dot{m}_{fluid\ tot} = \dot{m}_{fluid\ tot}(t-1) \cdot \left[K_P \cdot e(t-1) + K_D \cdot \frac{d[e(t-1)]}{dt}\right] \tag{3}$$

A comprehensive scheme is provided in Fig. 2. For every time-step, the control system computes the HTF mass flow rate according to the temperature error computed in the previous time-step and corrected by the use of the PD coefficients (Eq. 3). The transient thermal analysis is therefore made, and the error between target and obtained HTF outlet temperatures is evaluated and saved for the next control action (next time step).

As a further system optimisation, a suitable number of PD coefficients have been tested. High values of K_P and K_D are aim at keeping the HTF outlet temperature as close as possible to the target value even if this implies very aggressive corrective actions on the operating conditions of the pump. On the positive side, this case represents the safest case from a degradation perspective because excessive temperatures are avoided. On the contrary, low values of K_P and K_D provide a smoother control of $\dot{m}_{fluid\ tot}$ but they increase degradation due to large temperature gradients and high temperature peaks. Based on this, a third option is considered wherein variable under-relaxation factors are

used. In this more sophisticated control system, the actual value of these variable coefficients is assigned as a function of the error $e(t-1)$. When this error is low enough or when the actual temperature falls below a predefine safety margin, low gains are used to control the system as smooth as possible thus avoiding thermal and mechanical stress. On the other hand, when this limit is exceeded, the control system reacts assigning higher gains in order to re-establish the safety conditions from a fluid degradation perspective.

Two further conditions are still needed to define the controller completely. A lower temperature limit is introduced in order to avoid fluid solidification problems in case of long periods without heat supply; this limit is implemented by checking when the HTF at any location in the receiver is colder than the cold tank ($290°C$), at which point the receiver is emptied and an error message is displayed by the controller. A minimum temperature conditions is also set at the outlet of the receiver whereby if the HTF temperature is higher than $500°C$, then the fluid is allowed to enter the hot tank; otherwise, it is sent back to the cold tank. This condition is applied in order to safeguard the thermal conditions of the heat storage system; colder fluid coming in would cool the tank causing a drop in cycle efficiency.

The simulation results for the three cases are provided in Fig. 4, where overdamped and underdamped behaviors are easily identified. The outlet temperature for the *variable K case* presents important fluctuations which the control system is not able to attenuate, showing a visibly underdamped pattern. The *high K case* is similar though slightly less pronounced whilst the *low K case* is clearly overdamped (no fluctuations). With respect to working fluid degradation, i.e. the working fluid not exceeding $600°C$, only *variable K case* is compliant whilst the other two exceed this value and cause an irreversible deterioration of the molten salts. Moreover, *variable K* yields higher minimum temperature in the absence of heat supply, meaning that it is the system through which the conditions of the hot tank can be better preserved (stored fluid is not cooled down).

It is true that the capability to keep the temperature of the working fluid within a narrower range comes at the expense of very large flow gradients of the pumping system, which means that this system is definitely stressed out, in particular when the solar field is un-shadowed. Indeed, when the clouds leave, the incoming radiation rises from virtually zero to the rated value in just a few seconds, warming up the fluid to excessive temperatures. The impact on the pumping system and even its capability to follow this load changes will have to be investigated in a further work. Despite this, and with the information shown, the *variable K case* is considered the best solution.

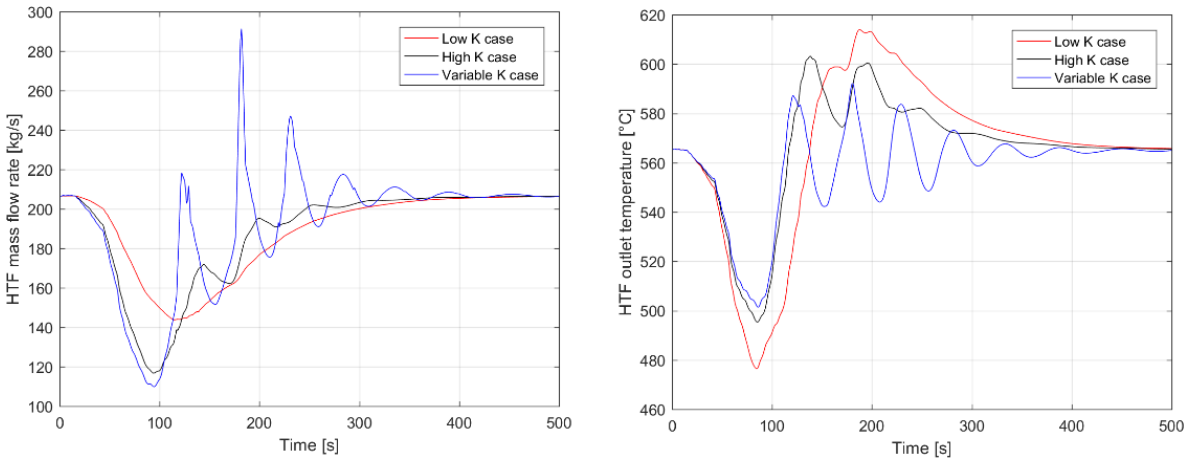

FIGURE 4. *Total Shadow as PS10* transient performance. *Feed-back* variants comparison: HTF mass flow (on the left) and HTF outlet temperature (on the right).

CONTROLLER COMPARISON: BACK VS. FORWARD

The proposed *feed-back* and *feed-forward* control methods are compared and analysed in this section. The comparison relies on three figures of merit considered: HTF mass flow rate, HTF outlet temperature and pipe wall temperature gradient.

With respect to pipe walls, the temperatures gradient to which the pipe surfaces are subjected are calculated in order to assess the corresponding thermal stress and identify critical locations. The maximum temperature gradient in the complete receiver surface is calculated for each time-step according to the following equation, which is applied to each location of the receiver (Eq. 4):

$$\frac{\partial T_{wall_{i,j,p}}}{\partial t} = \frac{T_{wall_{i,j,p}}(\tau) - T_{wall_{i,j,p}}(\tau - 1)}{t(\tau) - t(\tau - 1)} \tag{4}$$

Note that, by definition, the computed value is a *temporal* gradient, meaning that the temperature difference at a given location of the receiver is analysed between two consecutive time-steps. Furthermore, it has to be underlined that these results are strongly influenced by the quasi-steady state assumption for the pipe walls. In fact, not considering the thermal storage term and its damping function in energy equation of the pipe wall implies that the temperature gradient will be higher with respect to a fully transient thermal model incorporating all effects. As shown in Fig. 5, the models show a similar trend but the *feed-back* control system guarantees a lower maximum temperature gradient, yielding a reduction of more than $10°C/s$ with respect to the two *feed-forward* cases.

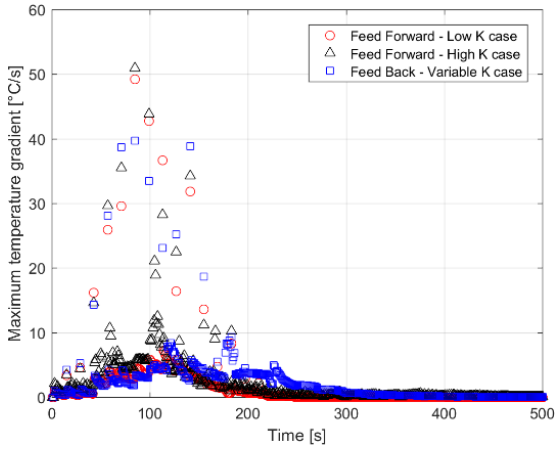

FIGURE 5. Transient performance for a *Total shadow as PS10* type of cloud. *Feed-back* vs. *Feed-forward* – Max pipe wall temperature gradient.

Further to the previous observation, the *feed-back* control method is the only one that complies with the maximum temperature limits. In fact, during the whole transient process, HTF that never exceed the degradation limit of $600°C$, hence preserving the thermal properties of the molten salts (Fig. 6). On the other hand, the *feed-forward* cases run the system into much riskier conditions with HTF temperatures close to $640°C$.

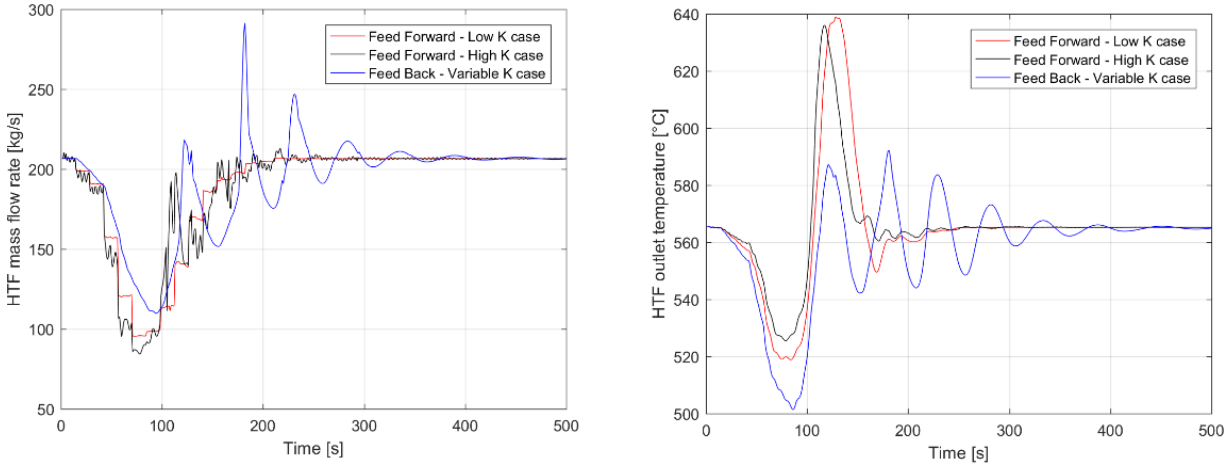

FIGURE 6. Transient performance for a *Total shadow as PS10* type of cloud. *Feed-back* vs. feed-*forward*: HTF mass flow (left) and HTF outlet temperature (right).

From an HTF mass flow rate perspective, the *feed-forward* cases present a similar trend due to the effects of a similar *lookup table* and the attenuation of the impact of the error. On the other hand, the *feed-back* case shows a more

oscillating trend with peak values in correspondence with the time-steps in which the system triggers corrective actions to control the strong temperature rise during the unshadowing phase. As a result of the explained characteristics, the *feed-back* case with variable *K* coefficients proves to be the best control system in order to guarantee safe operating conditions. Accordingly, the transient results shown in the rest of the document are obtained for this controller.

CLOUD COMPARISON

The transient model discussed in earlier sections is now used to analyze the performance of the system when subjected to cloud models considered, Fig. 1. To this aim, the Matlab code is launched with the radiation map (distribution of heat flux on the receiver surface) for each cloud. The main results are provided in Figs. 7 to 9.

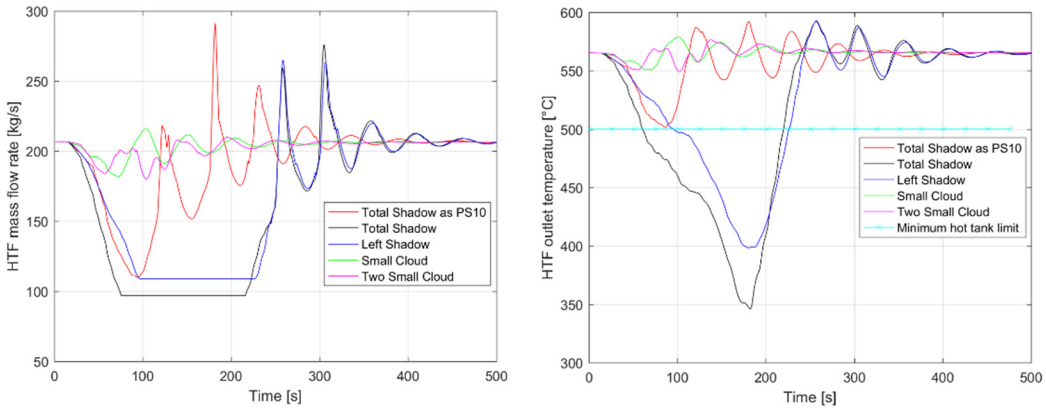

FIGURE 7. Cloud analysis. HTF mass flow rate (left), HTF outlet temperature (right).

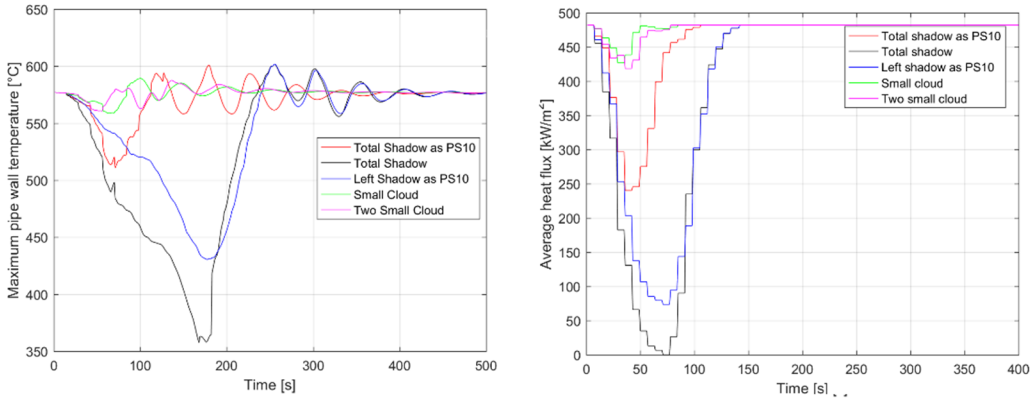

FIGURE 8. Cloud analysis. Maximum pipe wall temperature (left), average heat flux on the receiver (right).

From a thermal perspective, the *Total Shadow* cloud represents the most critical case. In fact, this cloud passage yields the highest temperature gradient in the receiver pipe walls and even brings about a trip of the system (production of hot molten salts ceases) due to absence of heat supply. This condition (no heat input at all in certain time steps) cools the system considerably, causing that the HTF be sent back to the cold tank. As a consequence, the controller takes no further actions and the mass flow rate is kept constant (horizontal line in Fig. 7, left). Fluid at constant temperature is circulated so as to ensure the shortest response time when heat supply becomes positive again in the unshadowing phase. When the solar field is un-shadowed, the boundary conditions change at a very fast rate and the control system has to properly manage the mass flow rate in order to avoid degradation issues even if at the cost of very large oscillations.

On the other hands, the *Small cloud* and the *Two small clouds* have the weakest impact on the system. Thanks to the heat capacity of the working fluid, the partial shadowing of the heliostats has a limited effect on the production of hot salts and, as a consequence, the total amount of HTF produced at the target temperature does not change proportionally to the reduction of heat supply with respect to the nominal value. Furthermore, the proportional relation

between radiation and temperature gradient is verified: the higher the radiation difference between two consecutive time steps, the higher the temperature gradient imposed on the receiver pipe walls. As a confirmation, the highest temperature gradient is observed for both the *Total shadow* and the *Left Shadow as PS10* cases, two clouds that introduce a complete shadowing of the solar field with radiation becoming null and then coming back to the nominal conditions and producing, as a consequence, the highest radiation gradient.

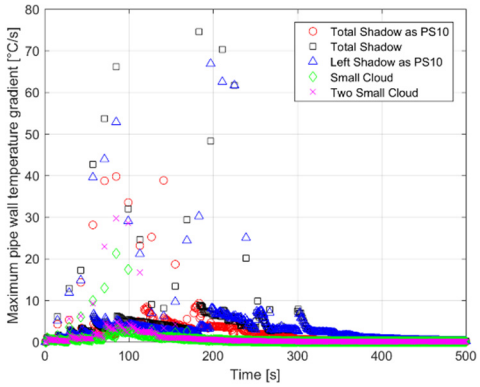

FIGURE 9. Cloud analysis – maximum pipe wall temperature gradient.

CONCLUSIONS

In this paper, different control strategies have been discussed in order to find to best solution to ensure the safe and efficient operation of a solar receiver. To this end, the chemical stability of the molten salts has been controlled by the preventing the HTF from exceeding its degradation temperature, whilst the mechanical integrity of the pipes is assessed through their local temperature gradients. Based on these figures of merit, three controllers have been compared: on one hand, two variants of a *feed-forward* control strategy, with low and high under-relaxation factor *K* respectively; on the other hand, a *variable K feed-back* strategy has also been considered. The analysis performed for the most critical clouds confirms that the latter is a better choice than any of the *feed-forward* options.

Indeed, the *feed-back* strategy is found to be the best solution for all the figures of merit taken into account. It results to be the unique strategy capable of avoiding HTF degradation, maintaining its outlet temperature under 600ºC. On the contrary, the HTF temperature increases up to 640 ºC with any of the *feed-forward* strategies. Moreover, the *feed-back* controller leads to a maximum temperature gradient on the receiver surface that is 20% lower than in both *feed-forward* variants, thus limiting the thermal stress in the material.

Finally, a comparison between the different types of clouds considered has been performed in order to identify the worst scenario and to test the control strategy of choice. The *Total Shadow* cloud emerges as the critical case as it yields higher peak temperatures and heat flux gradients than the other cloud schemes: from 6% higher than the *Left Shadow as PS10* to 80% higher than the *Small Cloud*. Moreover, the complete shadowing of the solar field brought about by the *Total Shadow* triggers the trip of the system, forcing the recirculation of the molten salts back to the cold tanks. Nevertheless, the *variable K feed-back controller* is able to handle this critical situation and the HTF temperature never exceeds the degradation temperature, not even at the beginning of the unshadowing process.

REFERENCES

1. Binotti, M., De Giorgi, P., Sánchez, D., & Manzolini, G. (2016). Comparison of Different Strategies for Heliostats Aiming Point in Cavity and External Tower Receivers. (ASME, A cura di) *Journal of Solar Energy Engineering, 138*, 021008-1 - 021008-11.
2. Crespi, F., & Zani, P. (2014). Best Aiming Strategy definition for off-design conditions due to passage of clouds in a Solar Tower. *Master Thesis.* Energy Engineering - Politecnico di Milano.
3. Toscani, A. (2017). Influence of clouds passing on the dynamic thermal performances of a tower receiver with heat storage system. *Master Thesis*. Energy Engineering - Politecnico di Milano.
4. Unbehauen, H. (2009). PID control. In *Control Systems, Robotics and Automation Vol. II: System Analysis and Control Classical Approaches* (p. 58-79). Oxford, UK: EOLSS Publishers Co.